

Variational Lang-Firsov approach plus Møller–Plesset perturbation theory with applications to *ab initio* polariton chemistry

Zhi-Hao Cui,^{1,*} Arkajit Mandal,¹ and David R. Reichman^{1,†}

¹*Department of Chemistry, Columbia University, 3000 Broadway, New York, NY 10027, United States*

(Dated: October 23, 2023)

We apply the Lang-Firsov (LF) transformation to electron-boson coupled Hamiltonians and variationally optimize the transformation parameters and molecular orbital coefficients to determine the ground state. Møller–Plesset (MP- n , with $n = 2$ and 4) perturbation theory is then performed on top of the optimized LF mean-field state to improve the description of electron-electron and electron-boson correlations. The method (LF-MP) is applied to several electron-boson coupled systems, including the Hubbard-Holstein model, diatomic molecule dissociation (H_2 , HF), and the modification of proton transfer reactions (malonaldehyde and aminopropenal) via the formation of polaritons in an optical cavity. We show that with a correction for the electron-electron correlation, the method gives quantitatively accurate energies comparable to exact diagonalization or coupled-cluster theory. The effect of multiple photon modes, spin polarization, and the comparison to the coherent state MP theory are also discussed.

I. INTRODUCTION

Electron-boson coupled systems have been a topic of interest in condensed matter physics for many decades [1–3]. The interaction between electrons and bosons, such as phonons and photons, can lead to the formation of quasiparticles, such as polarons and polaritons. A polaron is a quasiparticle consisting of an electron and its surrounding lattice deformation (phonons), whereas a polariton is a quasiparticle resulting from the strong coupling between matter excitations, such as excitons, and photons. Historically, the polaron problem has been a classic topic in condensed matter physics and plays a key role in various important phenomena, including charge transport (mobility), magnetism, and superconductivity [1, 4]. Recently, cavity-mediated chemical reactions have attracted renewed attention to polaritons, where experimental claims have been put forward that chemical reaction rates and pathways can be manipulated by the formation of polaritons in an optical cavity [5–12], potentially providing a new dimension for fine control of chemical processes [11, 13–16].

Theoretically, the study of electron-boson coupled problems involves both the study of model systems as well as the development of new computational methods to treat both model and *ab initio* systems. Several canonical lattice models have been proposed for the description of electron-phonon coupled systems [1], such as the Holstein, Su–Schrieffer–Heeger, and Fröhlich models. For realistic materials and molecules, an *ab initio* treatment is needed to predict material-specific properties. In such cases, an *ab initio* electronic Hamiltonian is usually augmented with a set of harmonic phonons/photons, which are linearly coupled to the electronic degrees of freedom [5, 12]. The boson frequencies are computed from *ab initio* calculations and the coupling strength is estimated by density functional perturbation theory or taken as input parameters from experiments. With respect to numerical method development, there has been significant progress in recent years which

describes the electronic and bosonic degrees of freedom on the same footing [5, 12, 17, 18]. These methods include density functional theory [19–24], QED quantum chemistry methods (including QED coupled cluster and their relatives) [25, 26], variational methods [27, 28], quantum Monte Carlo [29, 30], density matrix renormalization group (DMRG) [31, 32], diagrammatic and embedding-based approaches [33–35].

In this work, we aim to develop a numerical method that can handle both weakly and strongly coupled electron-boson coupled *ab initio* systems, while maintaining an economical computational cost. To this end, we utilize the (variational) canonical transformation to handle strong coupling effects and use perturbation theory to correct the missing electron-electron and electron-boson fluctuations. Our method is based on the Lang-Firsov (LF) transformation [36] for original electron-boson coupled Hamiltonians (similar ideas were used in Refs. [27, 37–43]). The boson degrees of freedom are then averaged out and the energy is variationally optimized. After the electronic determinant is calculated, the remaining electron-electron and electron-boson interactions are recovered by a Møller-Plesset (MP) perturbative treatment. This scheme is useful for determining the ground state of the coupled system and preserves a low computational complexity. For instance, second-order MP perturbation based on the transformed Hamiltonian has complexity of $\mathcal{O}(N_X N_{\text{orb}}^5)$, a product of the number of boson configurations N_X and the number of orbitals N_{orb} , which is potentially more efficient for large molecules or materials systems compared to more expensive QED-CCSD and higher-level approaches. The method starts from the canonical transformation and Hartree-Fock and therefore does not involve approximate density functionals and can be improved systematically.

The paper is organized as follows. In Sec. II, we introduce the model and a general *ab initio* electron-boson coupled Hamiltonian, the coherent-state based Hartree-Fock and MP perturbation theory, and then introduce the variational Lang-Firsov approach and its MP perturbative corrections. In Sec. III, we compute the ground-state properties of Hubbard-Holstein models and *ab initio* molecules coupled to an optical cavity. In particular, we discussed the classification of weak

* zhcu0408@gmail.com

† drr2103@columbia.edu

and strong coupling regions of the system, the multi-boson mode effect, and the role of symmetry-breaking reference. Finally, we summarize the main findings in Sec. IV.

II. MODEL AND METHOD

A. Electron-boson coupled Hamiltonian

A generic electron-boson coupled Hamiltonian can be written as,

$$\hat{H} = \underbrace{\sum_{pq\sigma} h_{pq} a_{p\sigma}^\dagger a_{q\sigma}}_{\hat{h}^{\text{el}}} + \frac{1}{2} \underbrace{\sum_{pqrs\sigma\tau} V_{pqrs} a_{p\sigma}^\dagger a_{r\tau}^\dagger a_{s\tau} a_{q\sigma}}_{\hat{v}^{\text{el}}} + \underbrace{\sum_x \omega_x b_x^\dagger b_x}_{\hat{h}^{\text{p}}} + \underbrace{\sum_x \sum_{pq\sigma} g_{pq}^x a_{p\sigma}^\dagger a_{q\sigma} (b_x + b_x^\dagger)}_{\hat{h}^{\text{el-p}}}, \quad (1)$$

where the fermion operator $a_{p\sigma}^\dagger$ creates an electron with spin σ at orbital p , and the boson operator b_x^\dagger creates a boson (phonon or photon) at mode x . h denotes the one-electron integral and V denotes the two-electron repulsion integral; ω is the frequency of boson and g is the electron-boson coupling tensor. We have assumed non-interacting bosons, which linearly couple to electrons.

In this work, we consider two special cases of Eq. (1). One is the *Hubbard-Holstein model*, which describes the interacting electrons in a lattice mediated by the phonon that couples to each site. The electronic part of the model (Hubbard part) approximates the one-electron integral as a single hopping value t and restricts the summation to the nearest neighbors in lattice sites,

$$h_{pq} = t\delta_{q,p+\eta}, \quad (2)$$

where η limits p and q to be neighboring sites. The two-electron integral is replaced by an on-site repulsion U , namely

$$V_{pqrs} = U\delta_{pq}\delta_{rs}\delta_{qr}. \quad (3)$$

For the phonon-related part, every phonon shares the same frequency $\omega_x = \omega$ and an electron-phonon coupling constant g ,

$$g_{pq}^x = g\delta_{xp}\delta_{pq}, \quad (4)$$

where the δ_{xp} means each phonon is locally attached to each lattice site.

The second Hamiltonian we discuss is an *ab initio* light-matter Hamiltonian, which describes a molecular system coupled to quantized radiation inside an optical cavity. In this work the light-matter interaction is described within the long-wavelength approximation, as is typically done, described by the Pauli-Fierz Hamiltonian in the dipole gauge [5, 44–46],

$$g_{pq}^x = -\sqrt{\frac{\omega_x}{2}} \lambda_c (\mathbf{e} \cdot \boldsymbol{\mu})_{pq}, \quad (5)$$

where λ_c is the coupling strength, \mathbf{e} is the polarization direction, and $\boldsymbol{\mu}$ is the molecular dipole integral,

$$\boldsymbol{\mu}_{pq} = \langle \phi_p | (\mathbf{r} - \sum_I Z_I \mathbf{R}_I) | \phi_q \rangle, \quad (6)$$

whose matrix element is the difference between the electronic and nuclear dipole (Z_I is the nuclear charge of atom I at position \mathbf{R}_I) in the one-particle basis $\{\phi\}$. Besides the coupling term, often one must include the dipole self-energies for each cavity mode in the dipole gauge [45, 47]. For this, each cavity mode included in the light-matter Hamiltonian contribute [48, 49]

$$\frac{1}{2} \left[\sum_{pq\sigma} \lambda_c (\mathbf{e} \cdot \boldsymbol{\mu})_{pq} a_{p\sigma}^\dagger a_{q\sigma} \right] \left[\sum_{rst} \lambda_c (\mathbf{e} \cdot \boldsymbol{\mu})_{rs} a_{r\tau}^\dagger a_{s\tau} \right] \quad (7)$$

to the electronic part of the original *ab initio* Hamiltonian. Then the modified one-electron integral reads,

$$h_{pq} = h_{pq}^{\text{kin}} + v_{pq}^{\text{nuc}} + \frac{1}{2} N_{\text{mode}} \lambda_c^2 \sum_r (\mathbf{e} \cdot \boldsymbol{\mu})_{pr} (\mathbf{e} \cdot \boldsymbol{\mu})_{rq}. \quad (8)$$

This includes the kinetic and nuclear-electron attractive potential, as well as the self-energy term of the cavity. Similarly, the two-electron integral is expressed as,

$$V_{pqrs} = V_{pqrs}^{\text{elec}} + N_{\text{mode}} \lambda_c^2 (\mathbf{e} \cdot \boldsymbol{\mu})_{pq} (\mathbf{e} \cdot \boldsymbol{\mu})_{rs}. \quad (9)$$

B. Coherent state Hartree-Fock and Møller-Plesset perturbation theory

The simplest mean-field wavefunction for electron-boson coupled systems is the product state of the electronic Slater determinant and the boson vacuum,

$$|\Phi\rangle = |\Phi^{\text{elec}}\rangle |0^{\text{p}}\rangle. \quad (10)$$

This wavefunction, however, does not account for the effect of electron-boson coupling. One way to incorporate the coupling is to introduce the origin shift of harmonic oscillators (with real coherent shifts $\{z_x\}$),

$$|\Phi^{\text{CS}}\rangle = \underbrace{\prod_x e^{-z_x (b_x - b_x^\dagger)}}_{\hat{U}^{\text{CS}}} |\Phi\rangle, \quad (11)$$

where \hat{U}^{CS} is the unitary transformation for displacements of bosons,

$$\hat{U}^{\text{CS}\dagger} b_x \hat{U}^{\text{CS}} = b_x + z_x. \quad (12)$$

This wavefunction ansatz is equivalent to applying the unitary transformation \hat{U}^{CS} to the Hamiltonian \hat{H} (Eq. (1), spin indices are ignored for simplicity)

$$\begin{aligned} \hat{H}^{\text{CS}} &= \hat{U}^{\text{CS}\dagger} \hat{H} \hat{U}^{\text{CS}} \\ &= \hat{H} + \sum_x \left[\omega_x z_x^2 + \sum_{pq} 2z_x g_{pq}^x a_p^\dagger a_q + \omega_x z_x (b_x + b_x^\dagger) \right]. \end{aligned} \quad (13)$$

In the transformed Hamiltonian, the oscillators are at new equilibrium positions, such that the wavefunction has the simple form $|\Phi\rangle$, and gives the same expectation value as $|\Phi^{\text{CS-HF}}\rangle$,

$$\begin{aligned} E &= \langle \Phi^{\text{CS-HF}} | \hat{H} | \Phi^{\text{CS-HF}} \rangle \\ &= \langle \Phi | \hat{U}^{\text{CS}\dagger} \hat{H} \hat{U}^{\text{CS}} | \Phi \rangle = \langle \Phi | \hat{H}^{\text{CS}} | \Phi \rangle. \end{aligned} \quad (14)$$

Under the stationary condition $\frac{\partial E}{\partial z_x} = 0$, z_x is determined by the one-electron density matrix $\gamma_{qp} = \langle a_p^\dagger a_q \rangle$,

$$z_x = - \sum_{pq} \frac{g_{pq}^x \gamma_{qp}}{\omega_x}. \quad (15)$$

This gives the expression for the coherent-state Hartree-Fock (CS-HF, or QED-HF) total energy,

$$E^{\text{CS-HF}}[\gamma, z(\gamma)] = E^{\text{HF}}(\gamma) + \sum_x \omega_x z_x^2. \quad (16)$$

Compared to the pure electronic HF theory, CS-HF modifies the electronic Fock matrix by adding the last term in Eq. (13),

$$F_{pq}[\gamma, z(\gamma)] = F_{pq}^{\text{elec}}[\gamma] + \sum_x 2z_x g_{pq}^x. \quad (17)$$

To formulate a self-consistent field (SCF) theory, the Fock matrix is diagonalized at each iteration to determine the molecular orbital (MO) energies (ε) and coefficients (C),

$$\sum_q F_{pq} C_{qm} = C_{pm} \varepsilon_m. \quad (18)$$

The one-electron density matrix γ is then constructed from the lowest N_{elec} occupied orbitals,

$$\gamma_{pq} = \sum_m^{\text{occ}} C_{pm} C_{mq}^\dagger. \quad (19)$$

The coherent shifts z 's are regarded as implicit variables, which are determined via Eq. (15) at each iteration. The new γ and z are used to construct the Fock matrix through Eq. (17) in the next iteration. At convergence, the density matrix γ is unchanged and the corresponding stationary condition of z is always satisfied.

Based on the CS-HF treatment, we can apply Møller-Plesset (MP) perturbation theory to obtain the correlation energy. Here, we briefly review the results from Refs. [26, 29]. The 0th order Hamiltonian is chosen as the Fock operator (Eq. (17)) with additional quadratic boson terms,

$$\hat{H}^{(0)} = \sum_{pq} F_{pq} a_p^\dagger a_q + \sum_x \omega_x z_x^2 + \sum_x \omega_x b_x^\dagger b_x. \quad (20)$$

The corresponding 0th order wavefunction is $|\Phi\rangle$,

$$\hat{H}^{(0)} |\Phi\rangle = E^{(0)} |\Phi\rangle, \quad (21)$$

with 0th order energy $E^{(0)} = \sum_m^{\text{occ}} \varepsilon_m + \sum_x \omega_x z_x^2$. Note that $E^{(0)}$ is different from the CS-HF energy in Eq. (16). The remaining part (namely, the fluctuation potential) is then,

$$\begin{aligned} \hat{W} &= \hat{H}^{\text{CS}} - \hat{H}^{(0)} = (\hat{V}^{\text{el}} - \hat{v}^{\text{HF}}) + \sum_x \omega_x z_x (b_x + b_x^\dagger) \\ &\quad + \sum_x \sum_{pq} g_{pq}^x a_p^\dagger a_q (b_x + b_x^\dagger). \end{aligned} \quad (22)$$

From Rayleigh-Schrödinger perturbation theory, The first-order perturbation energy is

$$E^{(1)} = \langle \Phi | \hat{W} | \Phi \rangle = E^{\text{HF}} - \sum_m^{\text{occ}} \varepsilon_m, \quad (23)$$

which recovers the CS-HF energy when added to $E^{(0)}$. For the coherent state second-order perturbation (CS-MP2), we have

$$E^{(2)} = - \sum_n \frac{|\langle \Phi_n^{\text{excited}} | \hat{W} | \Phi \rangle|^2}{E_n - E^{(0)}}. \quad (24)$$

The excited determinant may contain electronic or boson excitations. By applying the Slater-Condon rule, we have the expression

$$\begin{aligned} E^{(2)} &= - \frac{1}{4} \sum_{ijab} \frac{|\langle ij || ab \rangle|^2}{\varepsilon_a + \varepsilon_b - \varepsilon_i - \varepsilon_j} - \sum_x \sum_i \frac{|\omega_x z_x + g_{ii}^x|^2}{\omega_x} \\ &\quad - \sum_x \sum_{ia} \frac{|g_{ia}^x|^2}{\omega_x + \varepsilon_a - \varepsilon_i}, \end{aligned} \quad (25)$$

where i, j are occupied MO indices, and a, b are virtual MO indices. The first term includes the anti-symmetrized electron repulsion integrals in the MO basis $\langle ij || ab \rangle$, which comes from the electron-electron correlation (the same formula as standard MP2). The second term comes from pure boson excitations (the electronic part remains the ground-state determinant). This term, however, has no contribution if the stationary condition of z (Eq. (15)) is satisfied. Finally, the third term arises from a single-excited determinant coupled to a boson excitation. Higher-order excitations are zero due to the two-body nature of electron-electron interaction or the linear nature of electron-boson coupling.

C. Variational Lang-Firsov approach

We next use the following generalized version of the Lang-Firsov (LF) transformation,

$$\hat{U}^{\text{LF}} = \exp \left[\sum_{xp} \lambda_p^x a_p^\dagger a_p (b_x - b_x^\dagger) \right], \quad (26)$$

where λ_p^x are the variational parameters. This form of parametrization is used in the strong coupling QED-HF [43].

A more generic version that includes off-diagonal density coupling λ_{pq}^x is possible. However, the transformed Hamiltonian does not naturally truncate, and some approximation is needed. See Appendix A for further discussion.

One can perform the LF transformation on operators using

Baker–Campbell–Hausdorff (BCH) expansion,

$$\hat{U}^{\text{LF}\dagger} b_x \hat{U}^{\text{LF}} = b_x - \sum_p \lambda_p^x a_p^\dagger a_p, \quad (27)$$

$$\hat{U}^{\text{LF}\dagger} a_q \hat{U}^{\text{LF}} = a_q e^{\sum_y \lambda_q^y (b_y - b_y^\dagger)}. \quad (28)$$

After the CS and LF transformations, the Hamiltonian becomes,

$$\begin{aligned} \hat{H}^{\text{LF}} &= \hat{U}^{\text{CS}\dagger} \hat{U}^{\text{LF}\dagger} \hat{H} \hat{U}^{\text{LF}} \hat{U}^{\text{CS}} \\ &= \sum_{pq} h_{pq} e^{\sum_y (\lambda_q^y - \lambda_p^y) (b_y - b_y^\dagger)} a_p^\dagger a_q + \frac{1}{2} \sum_{pqrs} V_{pqrs} e^{\sum_y (\lambda_q^y - \lambda_p^y + \lambda_s^y - \lambda_r^y) (b_y - b_y^\dagger)} a_p^\dagger a_r^\dagger a_s a_q \\ &\quad + \sum_x \omega_x \left(b_x^\dagger + z_x - \sum_p \lambda_p^x a_p^\dagger a_p \right) \left(b_x + z_x - \sum_q \lambda_q^x a_q^\dagger a_q \right) \\ &\quad + \sum_{xpq} g_{pq}^x e^{\sum_y (\lambda_q^y - \lambda_p^y) (b_y - b_y^\dagger)} a_p^\dagger a_q \left(b_x + b_x^\dagger + 2z_x - 2 \sum_r \lambda_r^x a_r^\dagger a_r \right). \end{aligned} \quad (29)$$

After averaging over the zero-boson states, the Hamiltonian becomes,

$$\begin{aligned} \hat{H}^{\text{LF,elec}} &= \langle 0^{\text{P}} | \hat{H}^{\text{LF}} | 0^{\text{P}} \rangle \\ &= \sum_x \omega_x z_x^2 + \underbrace{\sum_{pq} \bar{h}_{pq} e^{-\frac{1}{2} \sum_y (\lambda_q^y - \lambda_p^y)^2} a_p^\dagger a_q + \sum_{xp} (\omega_x \lambda_p^x \lambda_p^x - 2\omega_x z_x \lambda_p^x) a_p^\dagger a_p}_{\hat{h}_1^{\text{eff}}} \\ &\quad + \frac{1}{2} \sum_{xpq} 2\omega_x \lambda_p^x \lambda_q^x a_p^\dagger a_q^\dagger a_q a_p - \frac{1}{2} \sum_{xpqr} 4g_{pq}^x \lambda_r^x e^{-\frac{1}{2} \sum_y (\lambda_q^y - \lambda_p^y)^2} a_p^\dagger a_r^\dagger a_r a_q \\ &\quad + \frac{1}{2} \sum_{pqrs} V_{pqrs} e^{-\frac{1}{2} \sum_y (\lambda_q^y - \lambda_p^y + \lambda_s^y - \lambda_r^y)^2} a_p^\dagger a_r^\dagger a_s a_q, \end{aligned} \quad (30)$$

where

$$\bar{h}_{pq} = h_{pq} + \sum_x 2z_x g_{pq}^x - \lambda_p^x g_{pq}^x - g_{pq}^x \lambda_q^x. \quad (31)$$

During the zero-boson averaging, we have used the Franck-Condon factors for the expectation value of the boson displacement operator in the boson-number basis [50],

$$\langle n | e^{-z(b-b^\dagger)} | m \rangle = \begin{cases} \sqrt{\frac{m!}{n!}} z^{n-m} e^{-\frac{z^2}{2}} L_m^{n-m}(z^2) & n \geq m \\ \sqrt{\frac{n!}{m!}} (-z)^{m-n} e^{-\frac{z^2}{2}} L_n^{m-n}(z^2) & n < m \end{cases} \quad (32)$$

where L_m^{n-m} is the associated Laguerre polynomials of degree m and order $n - m$. Physically, the transformation has two main effects: (1) It gives an exponential factor attached to one- and two-electron integrals, which makes their diagonal elements dominant; (2) It reduces the electron-electron repulsion (the penultimate term). In the strong coupling limit of the Hubbard-Holstein model, when $g \rightarrow \infty$, the effective U becomes negative.

The ground-state energy of Eq. (30) can be approximated by a single HF determinant, we call this the variational LF-HF method. The corresponding Fock operator can be defined normally using the transformed integrals,

$$\hat{F} = \sum_{pq} \hat{h}_1^{\text{eff}} + \hat{v}^{\text{HF}}. \quad (33)$$

The overall wavefunction is therefore parameterized by $\{\lambda_p^x\}$, $\{z_x\}$ and the orbital rotation between occupied and virtual blocks $\{\kappa_{ia}\}$,

$$\hat{U}^{\text{rot}} = \exp\left(\kappa_{ia} a_a^\dagger a_i - \kappa_{ia}^* a_i^\dagger a_a\right). \quad (34)$$

Unlike the CS-HF case, the λ parameters can not be determined analytically, and one has to variationally optimize them. The LF-HF energy reads,

$$E^{\text{LF-HF}} = \sum_x \omega_x z_x^2 + \text{Tr} \left[\left(\hat{h}^{\text{eff}} + \frac{1}{2} \hat{v}^{\text{HF}} \right) \gamma \right]. \quad (35)$$

For computational efficiency, the analytic gradients of LF-HF energy with respect to λ , z , and κ are derived in Appendix B and used during the optimization.

D. Lang-Firsov based Møller–Plesset perturbation theory

Similar to the CS-MP, one can formulate a Lang-Firsov Møller–Plesset (LF-MP) perturbation theory. We define the 0th-order Hamiltonian as the Fock matrix in the LF-HF approach (one can obtain the Fock matrix after optimization and canonicalize it to obtain orbital energies).

The fluctuation potential is again defined as the difference between \hat{H}^{LF} and $\hat{H}^{(0)}$,

$$\begin{aligned} \hat{W} = & \sum_x \omega_x z_x (b_x + b_x^\dagger) \\ & + \sum_{pq} \bar{h}_{pq} a_p^\dagger a_q \left[e^{\sum_y (\lambda_q^y - \lambda_p^y)(b_y - b_y^\dagger)} - e^{-\frac{1}{2} \sum_y (\lambda_q^y - \lambda_p^y)^2} \right] \\ & - \sum_{xp} \omega_x \lambda_p^x a_p^\dagger a_p (b_x^\dagger + b_x) \\ & + \sum_{xpq} g_{pq}^x a_p^\dagger a_q e^{\sum_y (\lambda_q^y - \lambda_p^y)(b_y - b_y^\dagger)} (b_x + b_x^\dagger) \\ & + \frac{1}{2} \sum_{xpq} 2\omega_x \lambda_p^x \lambda_q^x a_p^\dagger a_q^\dagger a_q a_p \\ & - \frac{1}{2} \sum_{xpqr} 4g_{pq}^x \lambda_r^x a_p^\dagger a_r^\dagger a_r a_q e^{\sum_y (\lambda_q^y - \lambda_p^y)(b_y - b_y^\dagger)} \\ & + \frac{1}{2} \sum_{pqrs} V_{pqrs} a_p^\dagger a_r^\dagger a_s a_q e^{\sum_y (\lambda_q^y - \lambda_p^y + \lambda_s^y - \lambda_r^y)(b_y - b_y^\dagger)} \\ & - \hat{v}^{\text{HF}}. \end{aligned} \quad (36)$$

Within this expression, there are more terms (with exponential displacement boson operators) than the CS-MP, and therefore the number of bosons in this approach may be extended to any value. In practice, one needs a truncation of the considered number of bosons N^b (typically, 10 bosons are enough to converge the energy). The rank of electronic excitation is still fixed as there is no higher-order interactions than two-body.

Similar to the CS-MP case, the first-order correction of the LF-MP theory gives exactly the LF-HF energy. The second-order perturbation is evaluated from the definition Eq. (24) and utilizes the Slater-Condon rules and Frank-Condon factors. For a collective boson configuration X , the phonon part of the fluctuation potential W can be integrated out (using Eq. (32)), and the electronic part is written in the occupied (i, j) and virtual (a, b) MO orbitals,

$$\begin{aligned} W(0, X) &= \langle \Phi^{\text{elec}} | \langle 0^b | \hat{W} | X \rangle | \Phi^{\text{elec}} \rangle, \\ W_i^a(0, X) &= \langle \Phi^{\text{elec}} | \langle 0^b | \hat{W} | X \rangle | \Phi_{ia}^{\text{elec}} \rangle, \\ W_{ij}^{ab}(0, X) &= \langle \Phi^{\text{elec}} | \langle 0^b | \hat{W} | X \rangle | \Phi_{ijab}^{\text{elec}} \rangle. \end{aligned} \quad (37)$$

The second-order correction (LF-MP2) is then computed as,

$$\begin{aligned} E^{(2)} = & - \sum_X \left[\frac{|W(0, X)|^2}{E_X} + \sum_{ia} \frac{|W_i^a(0, X)|^2}{\varepsilon_a - \varepsilon_i + E_X} \right. \\ & \left. + \sum_{ijab} \frac{|W_{ij}^{ab}(0, X)|^2}{\varepsilon_a + \varepsilon_b - \varepsilon_i - \varepsilon_j + E_X} \right], \end{aligned} \quad (38)$$

where the summation of boson configurations X are truncated according to the predefined maximum number of bosons. For each X , the computational cost is $\mathcal{O}(N_{\text{orb}}^5)$, the same as conventional MP2 theory. Every X is independent of each other and can be embarrassingly parallelized to reduce the additional factor N_X .

Similarly, one can evaluate the third- and fourth-order MP correction in the standard manner [51]. For example, the fourth-order correction is

$$\begin{aligned} E^{(4)} = & \sum_{s>0} \sum_{t>0} \sum_{u>0} \frac{W_{0s} \bar{W}_{su} \bar{W}_{ut} W_{t0}}{(E_0 - E_s)(E_0 - E_t)(E_0 - E_u)} \\ & - \sum_{s>0} \sum_{t>0} \frac{W_{0s} W_{s0} W_{0t} W_{t0}}{(E_0 - E_s)(E_0 - E_t)^2}, \end{aligned} \quad (39)$$

where

$$\bar{W}_{st} = W_{st} - \delta_{st} W_{00}, \quad (40)$$

and s, t, u are compound indices of electron and boson excitations. Note that the matrix element of $W(X, Y)$ may not be Hermitian when X and Y have different parity.

E. Computational details

The methods CS-HF, CS-MP, LF-HF, LF-MP, and exact diagonalization (ED) are implemented in the in-house program POLAR. Some of the electronic routines (such as the integral evaluations and SCF procedures) are combined with PySCF package [52, 53]. Both the spin-restricted (R) and spin-unrestricted (U) versions are implemented for comparison (see below).

The equilibrium bond lengths of H₂ and HF were taken as 0.746 Å and 0.918 Å. We used several bases (STO6G, 631G, 631**++G) for the diatomic molecules. The optimized geometries of malonaldehyde and aminopropenal were taken from Ref. [54]. The cc-pVDZ basis was used for the malonaldehyde and aminopropenal.

All calculations were converged to a change of energy smaller than 1×10^{-7} a.u.. The Lang-Firsov transformation for *ab initio* systems required a set of orthogonal bases (to avoid the inclusion of atomic overlap matrix), and we choose the meta-Löwdin orthogonalized orbitals [55] in the work. We use Broyden–Fletcher–Goldfarb–Shanno (BFGS) algorithm to minimize the LF-HF energy. The initial guess of parameters is taken from CS-HF or random values. For LF-MP, the maximum number of bosons is chosen as 16 (already converged for

the systems we considered). Furthermore, the boson configurations are parallelized using MPI. The DMRG calculations were performed using `BLOCK2` package [56, 57], which supported customized electron-boson Hamiltonians. The bond dimension was kept as 1000 for both electron and boson sites.

III. NUMERICAL RESULTS

A. Hubbard-Holstein models

We first benchmark the ground-state energy obtained from different methods in the 1D Hubbard-Holstein model. We consider a single electron on a 4-site Hubbard-Holstein model with different phonon frequencies (ω) and coupling strengths (g^2/ω); the results are collected in Fig. 1. Note that with a single charge this reduces the Hubbard-Holstein model to the pure Holstein one. Since the number of sites is small ($L = 4$), the ground state of the system can be found by exact diagonalization. In the adiabatic case (low frequency, $\omega = 0.1$, Fig. 1(a)), the LF-HF already gives a very accurate energy and naturally divides the coupling strength into two regimes: Before the slope changes ($g^2/\omega < 2$), the system is in the weak-coupling regime, whereas $g^2/\omega > 2$ defines the strong coupling regime. The CS-HF includes the correction from the coherent shift and CS-MP2 gives the perturbative correction on top of it. These two methods, however, do not capture the transition from the weak coupling to the strong coupling. In fact, they work well in the weak-coupling limit and provide a straight line of energy when g^2/ω increases. From the inset of Fig. 1(a), one can see that the LF-HF gives similar accuracy to CS-MP2 in the weak-coupling regime, and captures the transition of energy in the strong-coupling one. Since the LF-HF is already very accurate, the perturbative corrections are not evident in this case. From the inset of the figure, we can see that LF-MP2 and LF-MP4 further improve the energy description and provide very similar results to exact diagonalization (maximum error is about 0.01, 0.6% of the total energy).

We next discuss the physical interpretation of the LF approaches in Fig. 1(b), where $\omega = 0.5$. In this case, the weak-to-strong coupling transition happens around $g^2/\omega \sim 2.4$ and the LF-HF curve has a slope change. The error from LF-HF is larger than the model with $\omega = 0.1$ and is again similar to the error of CS-MP2 in the weak-coupling region. LF-MP2 and LF-MP4 are very accurate before the transition, but provide only small corrections after it. The error is maximized for the couplings just after the transition (largest error $\sim 2.6\%$) and becomes smaller again in the large coupling limit. Therefore, it is worth having a deeper look at the physical origin of the slope change and the different perturbative behaviors in the two regions. We plot the electronic density on each site ρ_i of the lattice for $g^2/\omega = 2.2$ and 2.4. One can clearly see that the charge density becomes non-uniform after the transition. This is due to the symmetry breaking of λ_p^x and z_x during the variational optimization. This can be viewed as the “self-trapping” of the polaron in the strong coupling limit [58], where the variationally optimal state is localized on a few sites

rather than spreading over the whole lattice. This symmetry breaking has a direct effect on the molecular orbital energy spectrum, which is also plotted in Fig. 1(b). In the weak-coupling region, the orbital energy obeys the symmetry of the model Hamiltonian and has a typical “diamond” shaped spectrum, i.e. the second and third orbitals are degenerate. On the other hand, after the symmetry breaking, the degeneracy no longer exists and the unoccupied energy levels are shifted up to higher energies. This makes electronic excitations less accessible and reduces the correlation energy from the perturbation (because most terms involve a sizable denominator associated with electronic excitations, for example in Eq. (38)). The LF-MP2 and LF-MP4 still provide some small corrections, but cannot recover the full correlation energy as they are low-order perturbations (see also Appendix A for the correlation energies from uniform density states). Thus, this symmetry breaking is spurious and can only be eliminated in a non-perturbative manner. Another perspective on this phenomenon is found via analogy to the symmetry-breaking methods in electronic structure theory. In an approximate variational method, symmetry breaking can happen to gain a lower energy at the cost of losing good quantum numbers. This is ubiquitous in the so-called “unrestricted” Hartree-Fock or Kohn-Sham density functional theory. For instance, the unrestricted HF breaks the spin S^2 symmetry but improves the energy of the dissociation curve of diatomic molecules (see Sec. III B for more details). Nonetheless, these symmetry-breaking approaches are often accompanied by the difficulty of including further corrections. The exact ground state shares the same symmetry as the Hamiltonian and starting from one particular symmetry-breaking reference, it is natural that the perturbative treatment would need high orders to recover the full symmetry of the system. Alternatively, one should regard the transition region as a strongly correlated problem and start with a multi-reference state (for example, from a multi-determinant ground state, which is a linear combination of symmetry-broken states and performs perturbation on top of it). We leave this topic to future work.

We finally discuss the 1D Hubbard-Holstein model with multiple electrons in Figs 1(c) and (d). We consider both adiabatic ($\omega = 0.5$) and anti-adiabatic ($\omega = 5.0$) cases. The initial guess of electron density is chosen as the antiferromagnetic (AFM) form. As shown in the figure, in the weak coupling regime, the converged spin density remains in an AFM pattern, i.e., the spin-up and spin-down densities are staggered on neighboring sites. After the transition to strong coupling, the electron-boson coupling is dominant and the converged spin densities are the same for different spin channels. Similar to the one-electron problem, the density is non-uniform in the strong coupling regime, although here the density is no longer localized at a single site. When boson frequency increases (anti-adiabatic case), the curve is shifted down in energy. And the error of the method with respect to exact diagonalization is also slightly smaller in the weak coupling regime. In the anti-adiabatic limit, the boson degrees of freedom can be integrated out and are thus more easily captured by the LF-HF.

When the on-site Coulomb interaction U increases from 2 to 4, the transition point from weak to strong coupling is

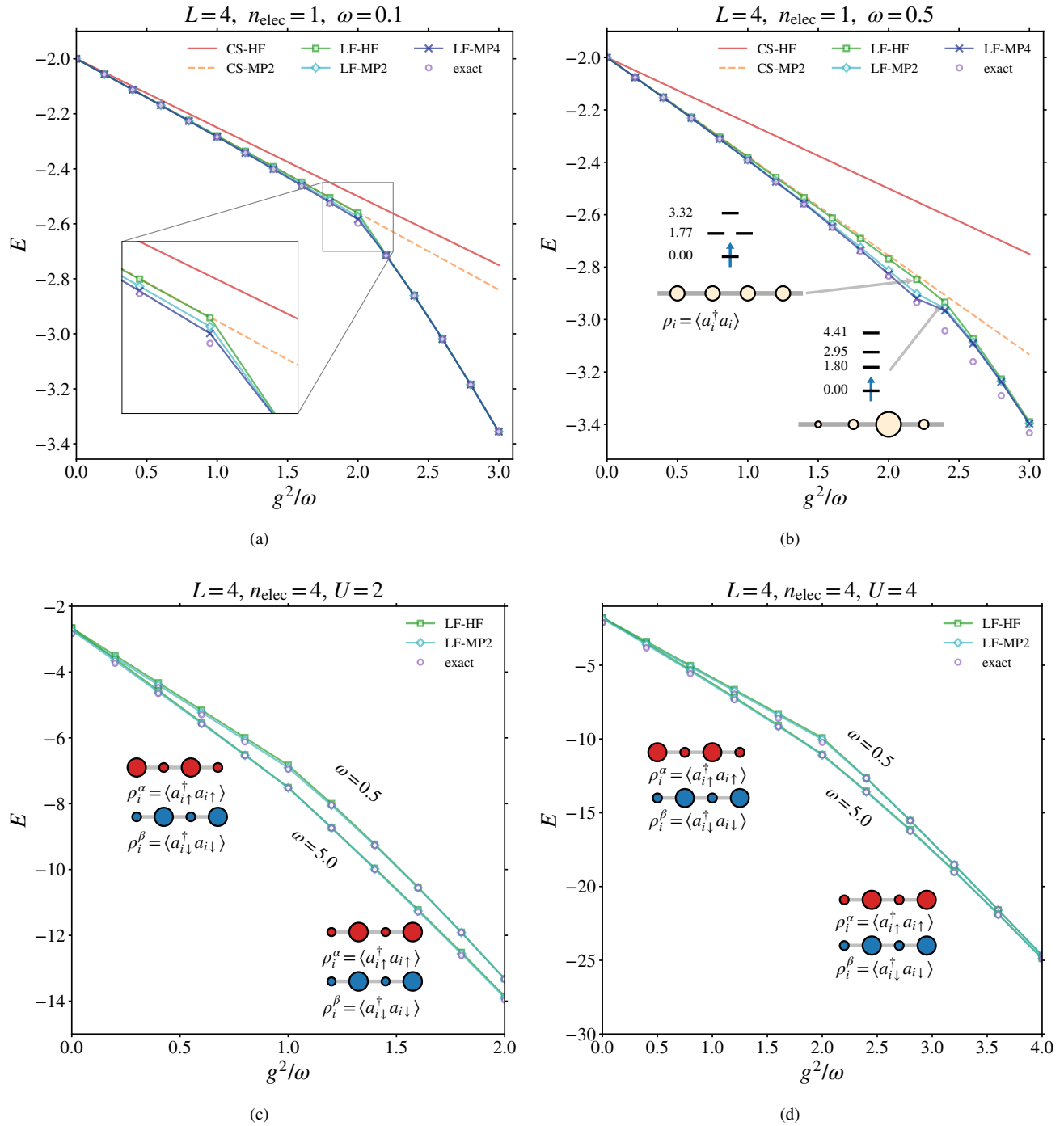


FIG. 1. Ground-state energy of the 1D Hubbard-Holstein model, for different coupling strengths g^2/ω . The periodic lattice size L is taken as 4. (a) $\omega = 0.1$, one electron. (b) $\omega = 0.5$, one electron. The electron densities ρ_i at site i and molecular orbital energies (relative to the lowest energy) are shown for the two coupling values (2.2 and 2.4) around the self-trapping transition. (c) 4 electrons with on-site interaction $U = 2$. (d) 4 electrons with on-site interaction $U = 4$.

postponed until approximately $g^2/\omega = 2.0$. Since the U value is larger, the symmetry-breaking mean field favors the AFM state more, and the electron-boson interaction is less effective at redistributing the spin density pattern. Since $U = 4$ is not very large, we expect the MP2-level treatment to work well

for the cases. When the electron-electron repulsion becomes extremely large, such as $U > 10$, LF-MP2 would break down in the weak coupling regime, but may still work in the strong-coupling one since the electron-boson interaction reduces the effective U .

B. Diatomic molecules coupled to photons

Next, we benchmark the ground-state energy of diatomic molecules coupled to cavity photons with our methods. The Hamiltonian takes the form of Eqs. (5)-(9). To compare with the energies from ED/DMRG or QED-CCSD, we need to add a correction term from the missing energy of electron-electron interactions,

$$\Delta E^{\text{corr}} = E^{\text{CCSD(T) or CCSD}}[\Phi^{\text{elec}}] - E^{\text{MP2}}[\Phi^{\text{elec}}], \quad (41)$$

where Φ^{elec} is the ground-state electronic Slater determinant from CS-HF or LF-HF and this correction is added to the CS-MP2 or LF-MP2 energy.

The photon frequencies are chosen to match the first electronic excited energy ω_0 of the corresponding molecule,

$$\omega_x = (2x + 1)\omega_0, \quad x = 1, 2, \dots, N^{\text{mode}}, \quad (42)$$

where for hydrogen (H_2) $\omega_0^{\text{H}_2} = 0.466751$ a.u. and for hydrogen fluoride (HF) $\omega_0^{\text{HF}} = 0.531916$ a.u.. The coupling constant λ_c is chosen as 0.05 and 0.5 a.u. to assess medium and strong coupling situations respectively.

We first consider a single photon mode with an intermediate coupling $\lambda_c = 0.05$ a.u., as shown in Fig. 2 (a). The CS-HF and LF-HF energetics behave similarly for the H_2 and HF molecules. In these cases, the MP2 corrections are also similar. After adding the electronic correction (Eq. (41)), the errors from CS-MP2 and LF-MP2 are all within the chemical accuracy (< 1 kcal/mol). This reflects that these systems can be classified as weakly coupled problems (similar to the HH models with a small coupling constant), and are therefore very well described by CS-MP2 and LF-MP2. When more photon modes are considered (Fig. 2(b)), the two methods are still similar and their errors are within the chemical accuracy.

The large coupling case ($\lambda_c = 0.5$ a.u.), on the other hand, has larger errors for all methods. In particular, we see substantial improvements in LF-HF over CS-HF, and LF-MP2 over CS-MP2. For example, for H_2 in 631G with 1 photon mode, the CS-MP2 with the correlation correction gives an error of -21.3 kcal/mol while LF-MP2 with the correction gives an error of 2.6 kcal/mol. This suggests that in the strong-coupling regime, the LF-type approaches are more accurate than the coherent-state-based ones. The difference between LF-HF and CS-HF can be regarded as a signal of strong coupling and large deviations indicate the degradation of the CS-based methods.

Furthermore, when more photon modes are included, the error also becomes larger, and in such cases, the LF-type approaches also provide larger improvements. In contrast to the intermediate coupling case, as the coupling becomes strong, the multi-mode effect becomes important and the single-mode approximation is no longer valid. One needs to develop methods that explicitly include the higher photon modes with the awareness that such problems are potentially more strongly correlated.

We finally discuss the dissociation of diatomic molecules in a photon cavity ($\lambda_c = 0.05$ a.u.), as shown in Fig. 4. In the H_2

case, restricted (R) CS-HF performs similarly to regular HF, which does not capture the radical nature in the dissociation limit and thus exhibits a blow-up in energy. The unrestricted (U) HF does not break symmetry near the equilibrium geometry and overlaps with the RCS-HF. In the dissociation limit, the UCS-HF provide an accurate energy at the cost of breaking $\text{SU}(2)$ S^2 symmetry, which is well-known in quantum chemistry. The perturbative correction on top of the unrestricted reference then gives an accurate description of the whole curve. Interestingly, the RLF-MP2 + CCSD electronic correction (Eq. (41)) gives almost exact results, whereas the RCS-MP2 + CCSD correction is lower in energy in the dissociation limit. Since CCSD is exact for 2-electron systems, the error is likely from the electron-photon coupling part, and this reflects that the reference in the RCS-MP2 is not good enough for a low-order perturbative treatment of electron-photon interactions here.

In Fig. 4 (b), the dissociation of HF molecule shows similar trends as those in H_2 molecule. Again, all curves overlap in the equilibrium region and deviate when the bond is stretched. The unrestricted references are expected to be good in the dissociation limit and hence give a flat result. The restricted reference, however, is not good for both electron-electron and electron-photon interactions in such a limit. The restricted curves are then shifted up a bit in energy, and the RLF-MP2 is slightly better than RCS-MP2.

C. Proton-transfer reaction barriers

In this section, we consider two more realistic *ab initio* systems and focus on the reaction barrier of proton-transfer reactions when they are coupled to optical cavities.

Malonaldehyde is a prototypical molecule in the study of proton transfer. It is symmetric with respect to the reactant (R) and product (P). When the polarization direction is along the x axis (Fig. 5 (a)), the existence of photons and their coupling to electrons increase the reaction barrier, which can be seen from the CS-HF/LF-HF versus the bare HF curve. The electron-electron correlation, on the other hand, reduces the reaction barrier. The MP2 and CCSD corrections lower the barrier by about 6 and 4 kcal/mol, respectively. In particular, the MP2 underestimates the barrier significantly and highlights the necessity of the correction term for the electron-electron interactions. Nevertheless, the electron-photon coupling only needs an MP2 level of theory. As we can see clearly from Fig. 5(a), the CS-MP2 and LF-MP2 with electronic correction provide very similar barriers compared to the reference value from QED-CCSD-22 [54] (error < 1 kcal/mol). The similarity between CS and LF theories also suggests that the system should be within the weak-coupling region. When the polarization direction is along the z axis (Fig. 5 (b)), the electron-photon coupling shifts the barrier only slightly, and other properties are similar to the case along the x axis.

The Aminopropenal molecule is asymmetric with respect to reactants and products. The results are collected in Fig. 6. For the reaction barrier, the observations are similar to those observed with malonaldehyde. Here, CS-HF and LF-HF also

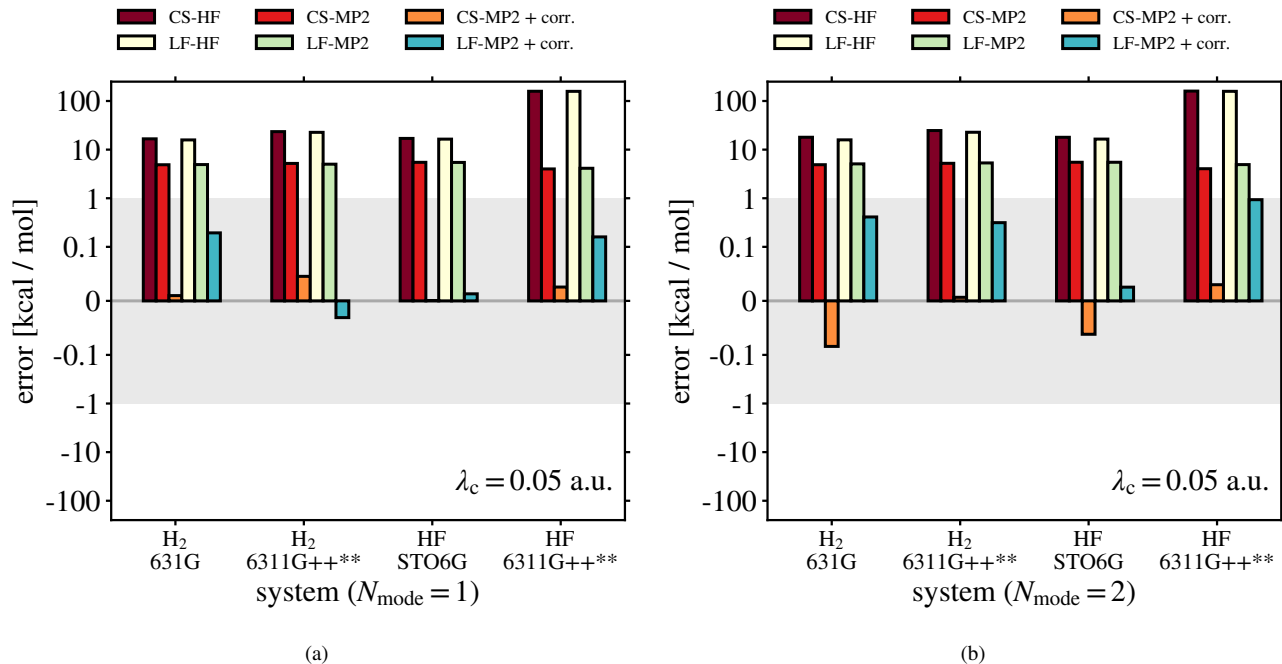


FIG. 2. Error in energy of diatomic molecules H₂ and HF in the medium-coupling regime ($\lambda_c = 0.05$ a.u.). The reference energies of H₂ are from exact diagonalization (ED) or DMRG (DMRG is used for the HF with 6311G+** basis). The shaded area labels chemical accuracy (error < 1 kcal/mol).

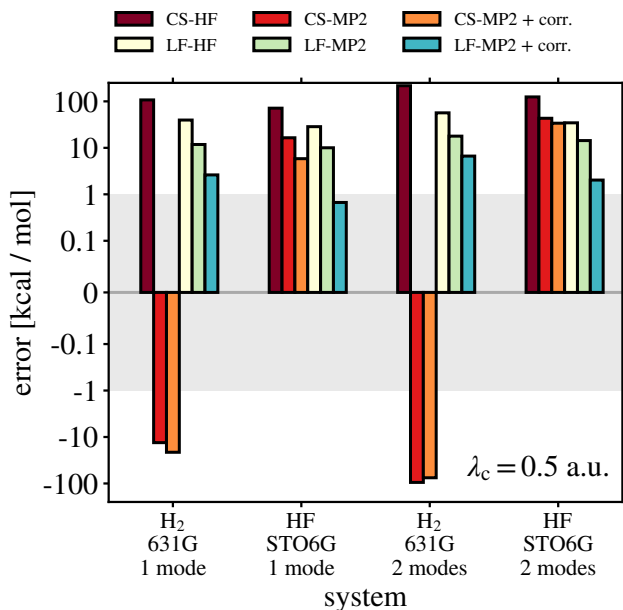


FIG. 3. Error in the energy of diatomic molecules H₂ and HF in the strong-coupling regime ($\lambda_c = 0.5$ a.u.). The reference energies are from exact diagonalization. The shaded area labels the chemical accuracy (error < 1 kcal/mol).

overestimate the reaction energy ($E_P - E_R$), which is corrected by correlation terms. The LF-based methods are slightly better

in the description of the reaction energy than the CS-based methods.

IV. CONCLUSIONS

In summary, we developed a Lang-Firsov transformation-based perturbation scheme for electron-boson coupled problems. The method relies on the variational optimization of Lang-Firsov and coherent parameters for a zero-boson averaged electronic Hamiltonian, and the subsequent use of a Möller-Plesset perturbative treatment for electron-boson couplings.

As shown in the cases of the Hubbard-Holstein model and *ab initio* molecules (diatomic molecules and proton transfer reaction barriers coupled to a photon cavity), the LF-based methods perform well for weakly-coupled systems and strongly-coupled limits. The methods provide a natural interpolation between the two limits. The comparison between CS and LF-based approaches is useful for identifying the transition to the strong electron-boson couplings regime, and in these systems, the LF-based methods are preferred. When the coupling constant becomes extremely large or when multi-boson modes are involved, the CS-based methods should be used with caution, and a more generalized Lang-Firsov transformation may be useful for capturing the non-diagonal effects.

In the intermediate coupling region, the LF-MP scheme may underestimate the correlation energy due to the symmetry-breaking from the variational optimization. This is in principle

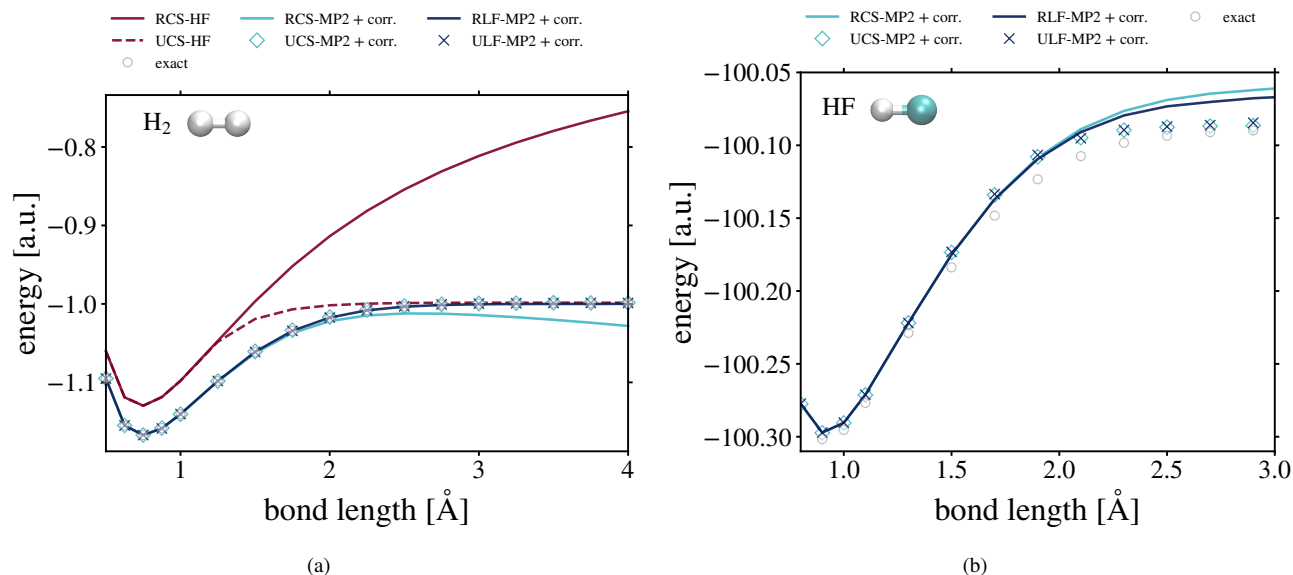


FIG. 4. Dissociation of diatomic molecules H₂ and HF in a photon cavity ($\lambda_c = 0.05$ a.u.). Both spin-restricted (R) and unrestricted (U) determinants are considered.

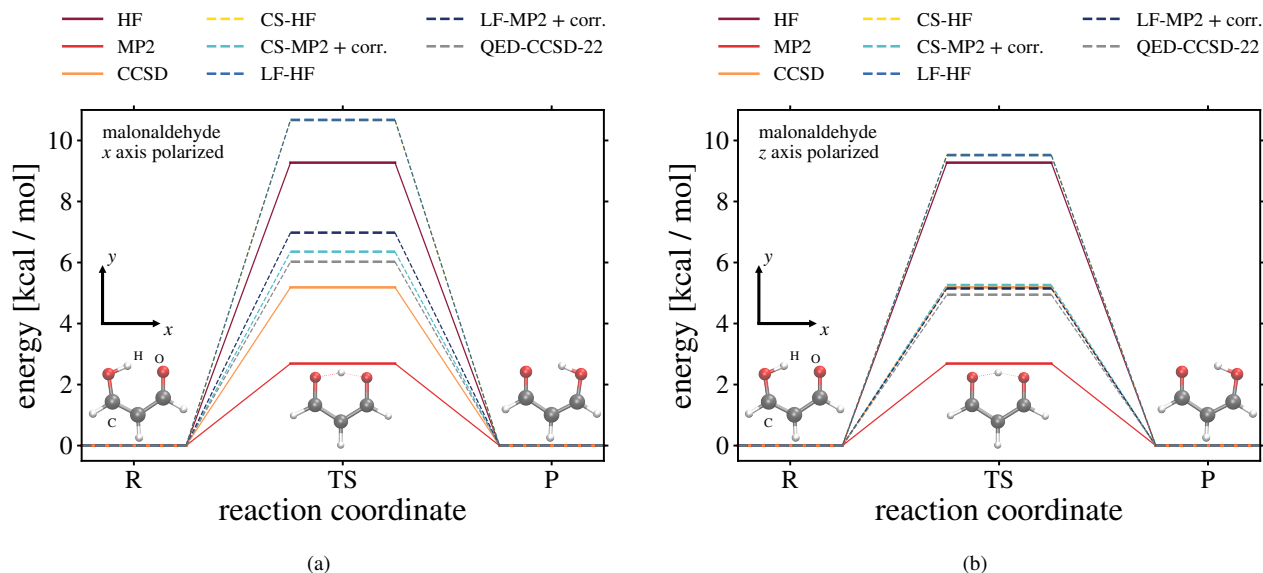


FIG. 5. Proton transfer in malonaldehyde inside and outside of a cavity. Only one photon mode is considered with $\omega_0 = 3$ eV and $\lambda_c = 0.1$ a.u. The HF, MP2, CCSD are methods without photon (and coupling) terms. QED-CCSD-22 is taken from Ref. [54]. The polarization direction is along (a) the x axis and (b) the z axis.

a multi-reference problem, and a CI-based or multi-reference-based perturbation theory should be used. Another possibility is to introduce a symmetry-breaking electronic reference. As shown by the dissociation curve of the diatomic molecules, a spin-symmetry breaking reference improves the overall energy description. Other types of symmetry-breaking schemes are possible and may be useful for condensed matter systems (such as a Bardeen–Cooper–Schrieffer reference for superconductors coupled to phonons or photons). We plan to explore

these and related directions in future works.

ACKNOWLEDGMENTS

We thank Garnet Chan, Ankit Mahajan, Junjie Yang, Huanchen Zhai, and Chong Sun for the helpful discussions. ZHC was funded by the Columbia MRSEC on Precision-Assembled Quantum Materials (PAQM) under award number

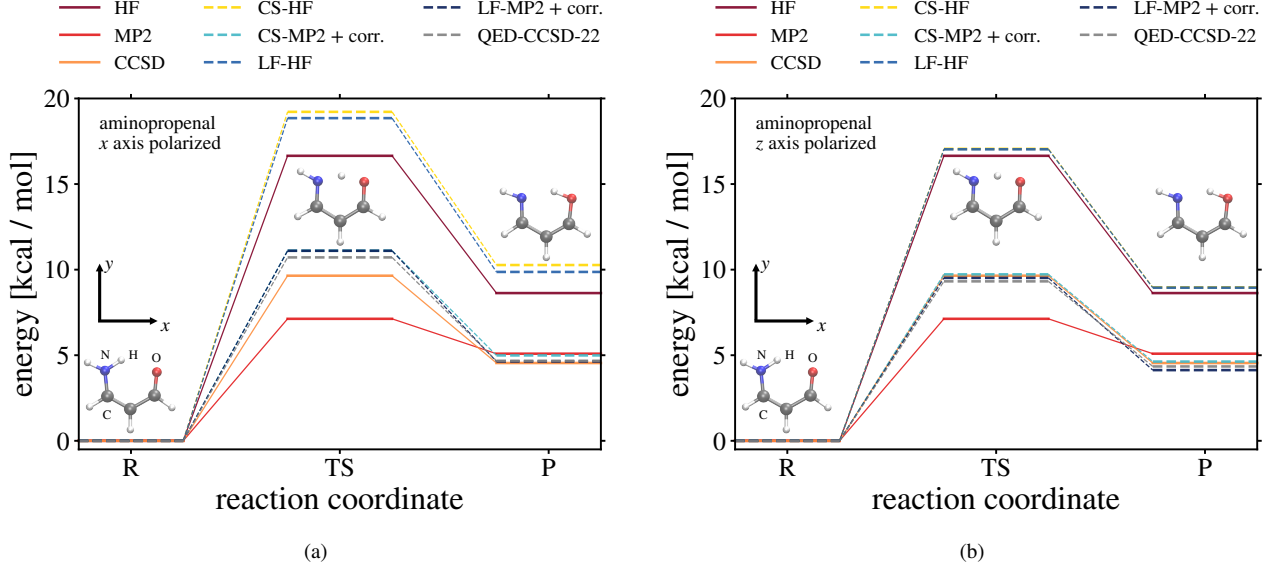


FIG. 6. Proton transfer in aminopropenal inside and outside of a cavity. Only one photon mode is considered with $\omega_0 = 3$ eV and $\lambda_c = 0.1$ a.u. The HF, MP2, and CCSD are methods without photon (and coupling) terms. QED-CCSD-22 is taken from Ref. [54]. The polarization direction is along (a) the x axis and (b) the z axis.

DMR-2011738.

Appendix A: Uniform and generalized Lang-Firsov transformation

Here, we discuss other possible forms of Lang-Firsov transformation.

The simplest version is the uniform version (the original parametrization in the Ref. [36]), where every site in the Hubbard-Holstein model shares the same scalar value of λ and z , which we call *uniform LF*. The results are shown in Fig. 7. It can be seen that in the weak coupling regime, there is no symmetry breaking, and the uniform LF and LF are almost identical. In the $\omega = 0.1$ case, the uniform MP follows roughly a straight line, which does not capture the slope change. While in the $\omega = 0.5$ case, the uniform LF-MP behaves better near the transition point around $g^2/\omega = 2.2$. This result reflects that in the strongly coupling region, a perturbation starting from a symmetry-preserved state may give larger corrections, and in some cases (such as the intermediate coupling region at $\omega = 0.5$), the uniform LF-MP gives better results.

A more *general Lang-Firsov (GLF)* transformation, which includes coupling to a non-diagonal electronic density, is

$$\hat{U}^{\text{GLF}} = \exp \left[\sum_{xpq} \lambda_{pq}^x a_p^\dagger a_q (b_x - b_x^\dagger) \right]. \quad (\text{A1})$$

One can use the BCH expansion to obtain the effect of this transformation on boson operators,

$$\hat{U}^{\text{GLF}\dagger} b_x \hat{U}^{\text{GLF}} = b_x - \sum_{pq} \lambda_{pq}^x a_p^\dagger a_q. \quad (\text{A2})$$

The transformation of the electron operator, on the other hand, involves the combination of all other operators,

$$\hat{U}^{\text{GLF}\dagger} a_q \hat{U}^{\text{GLF}} = \sum_p \left[e^{\sum_y \lambda_{pq}^y (b_y - b_y^\dagger)} \right]_{qp} a_p. \quad (\text{A3})$$

The transformed Hamiltonian after zero-boson averaging can be expressed in the BCH expansion (up to $2N$ -th order),

$$\hat{H}^{\text{GLF,elec}} = \langle 0^p | \hat{U}^{\text{GLF}\dagger} \hat{H} \hat{U}^{\text{GLF}} | 0^p \rangle. \quad (\text{A4})$$

The Hamiltonian elements are

$$H^{\text{GLF}} = \sum_{n=2}^{2N} (-1)^N \frac{n_{x_1}!! \cdots n_{x_n}!!}{n!} \sum_{x_1, x_2, \dots, x_n}^{\text{all strings of order } n} \times [\cdots [H, \lambda^{x_1}], \dots, \lambda^{x_{n-1}}] \lambda^{x_n}, \quad (\text{A5})$$

where the one-body and two-body commutators are defined as,

$$[h, \lambda^x]_{pq} = (h \cdot \lambda^x - \lambda^x \cdot h)_{pq}, \quad (\text{A6})$$

$$[V, \lambda^x]_{pqrs} = \sum_m (V_{pmrs} \lambda_{mq}^x + V_{pqrm} \lambda_{ms}^x - V_{mqrs} \lambda_{mp}^x - V_{pqms} \lambda_{mr}^x). \quad (\text{A7})$$

The BCH expansion in Eq. (A5), however, only converges when λ is small, and the number of boson strings scales exponentially. Thus, it is not practical to apply.

One approximation proposed in Refs. [59, 60] is to assume λ 's of different mode x commute with each other, and this

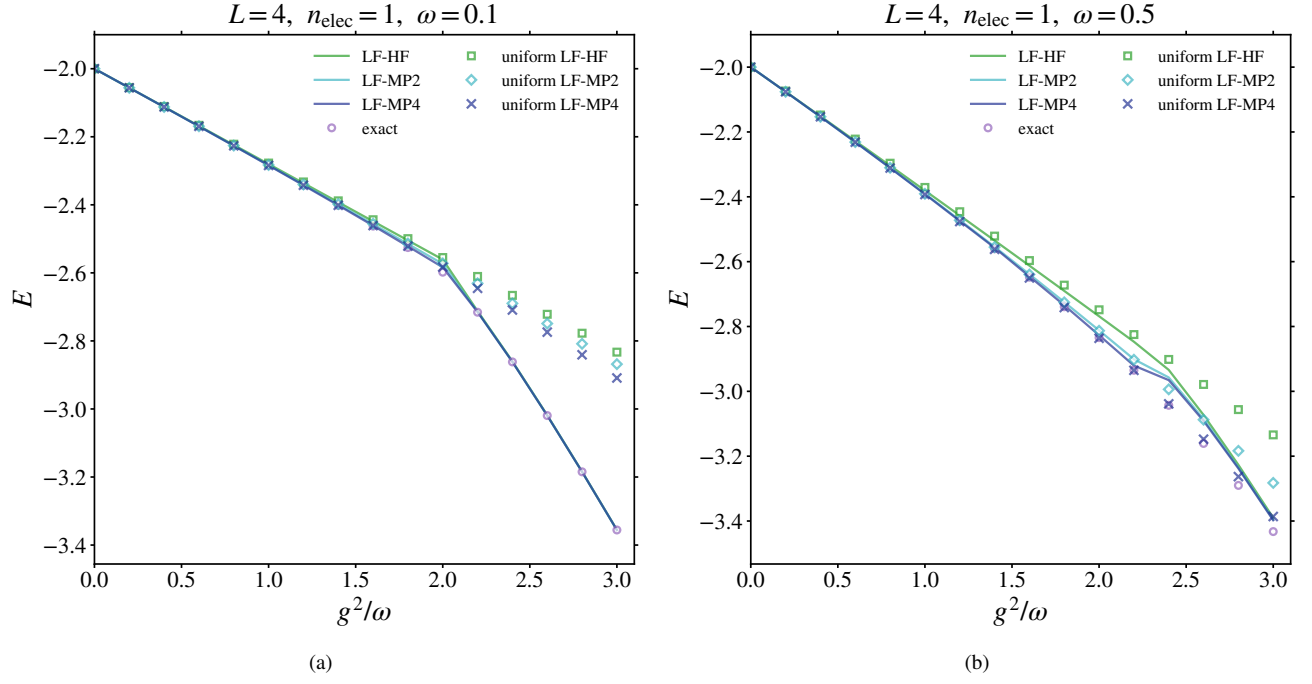


FIG. 7. The uniform version of LF transform is compared to the non-uniform one (λ vs. λ_p^x), with two different model frequencies (a) $\omega = 0.1$ and (b) $\omega = 0.5$.

leads to a simplification of the nested commutator and can be evaluated to the infinite order such that the restriction on small λ is relaxed.

$$h_{pq}^{\text{GLF}} = \sum_{ij} (e^\Lambda)_{pq,ij} h_{ij}, \quad (\text{A8})$$

$$V_{pqrs}^{\text{GLF}} = \sum_{ijkl} (e^\Lambda)_{pqrs,ijkl} V_{ijkl}, \quad (\text{A9})$$

where Λ is defined as the double commutator operator, whose action on a Hamiltonian H is defined as

$$\Lambda H = -\frac{1}{2} [[H, \lambda^x], \lambda^x]. \quad (\text{A10})$$

Note the Eq. (A9) formally has computational complexity $\mathcal{O}(N_{\text{orb}}^8)$ as well as a impractical storage of a very large $\mathcal{O}(N_{\text{orb}}^8)$ exponential tensor. This bottleneck can be circumvented by the algorithm of computing the action of a matrix exponential on a vector [61], which does not require the explicit build of the $\mathcal{O}(N_{\text{orb}}^8)$ tensor. By using such an algorithm, only several evaluations of the double commutator (Eq. (A10)) are needed, and thus scales only $\mathcal{O}(N_{\text{orb}}^5)$. Furthermore, the storage is only $\mathcal{O}(N_{\text{orb}}^4)$.

In Table I, we compare the performance of uniform LF, LF, and GLF on the Hubbard-Holstein model and H_2 molecule in a cavity.

In the Holstein model, because of the special local structure of the electron-phonon coupling tensor (Eq. (4)), the improvement from the non-local coupling (GLF) is marginal (the

TABLE I. Comparison of uniform LF, LF, and generalized LF (GLF) transformation. The systems include the Hubbard-Holstein (HH) models ($\omega = 0.5$) with one electron, and the H_2 molecule (in 631G basis with a different coupling constant λ_c). The energies/coupling constant for *ab initio* systems are in the unit of a.u. The uniform LF-HF is meaningless for *ab initio* systems since the orbitals are not translational invariant.

System	CS-HF	LF-HF	LF-HF uniform	GLF-HF
HH model ($\frac{g^2}{\omega} = 1.0$)	-2.2500	-2.3711	-2.3807	-2.3808
HH model ($\frac{g^2}{\omega} = 2.4$)	-2.6000	-2.9016	-2.9339	-2.9435
H_2 (1 mode, $\lambda_c = 0.05$)	-1.1239	-	-1.1252	-1.1253
H_2 (1 mode, $\lambda_c = 0.5$)	-0.8710	-	-0.9790	-0.9904
H_2 (2 modes, $\lambda_c = 0.05$)	-1.1212	-	-1.1245	-1.1246
H_2 (2 modes, $\lambda_c = 0.5$)	-0.6432	-	-0.8991	-0.9244

correction is slightly larger for the stronger coupling case, $g^2/\omega = 2.4$).

For the H_2 molecule with a small coupling constant $\lambda_c = 0.05$, the energy from GLF-HF is only slightly lower than that from LF-HF. The two solutions are almost identical. For the large coupling $\lambda_c = 0.5$, however, the correction from GLF is larger. As discussed in the main text, the multi-mode effect increases the correlation energy of electron-photon coupling. Such a strongly coupled system naturally has larger correction from a larger variational space. In general, for *ab initio* systems, the electron-boson coupling tensor is no longer diagonal. Although in this work LF-MP2 (with an electronic correlation correction) appears to already work well for most

systems, a generalized transformation is expected to be useful for extremely strongly coupled systems.

Appendix B: Analytical gradient of variational Lang-Firsov approach

By applying the chain rule to the LF-HF energy (Eq. (35)), one can compute its gradient with respect to variational parameters.

The gradient of coherent shifts z_x is,

$$\frac{\partial E}{\partial z^y} = 2\omega_y z_y + 2 \sum_{pq} g_{pq}^y e^{\Lambda_{pq}} \gamma_{qp} - 2 \sum_p \omega_y \lambda_p^y \gamma_{pp}, \quad (\text{B1})$$

where we defined the shorthand notations,

$$\Lambda_{pq} = -\frac{1}{2} \sum_y (\lambda_q^y - \lambda_p^y)^2, \quad (\text{B2})$$

$$\Lambda_{pqrs} = -\frac{1}{2} \sum_y (\lambda_q^y + \lambda_s^y - \lambda_p^y - \lambda_r^y)^2. \quad (\text{B3})$$

The (spin-restricted) gradient of LF parameters λ_{pq}^x are (Ein-

stein summation is assumed for clarity),

$$\begin{aligned} \frac{\partial E}{\partial \lambda_m^y} &= 2\lambda_p^y h_{pq}^{\text{eff}} e^{\Lambda_{pq}} \gamma_{qm} - 2\lambda_m^y h_{pq}^{\text{eff}} e^{\Lambda_{pq}} \gamma_{qm} \\ &\quad - 2g_{pq}^y e^{\Lambda_{pq}} \gamma_{qp} + 2\omega_y \lambda_m^y z_y \gamma_{mm} \\ &\quad + 2\omega_y \lambda_q^y \gamma_{qq} \gamma_{mm} - \omega_y \lambda_q^y \gamma_{mq} \gamma_{mq} \\ &\quad - 2V_{pmrs} e^{\Lambda_{pmrs}} \lambda_m^y \gamma_{mp} \gamma_{sr} + V_{pmrs} e^{\Lambda_{pmrs}} \lambda_m^y \gamma_{ps} \gamma_{mr} \\ &\quad + 2V_{pmrs} e^{\Lambda_{pmrs}} \lambda_p^y \gamma_{mp} \gamma_{sr} - V_{pmrs} e^{\Lambda_{pmrs}} \lambda_p^y \gamma_{ps} \gamma_{mr} \\ &\quad - 2V_{pmrs} e^{\Lambda_{pmrs}} \lambda_s^y \gamma_{mp} \gamma_{sr} + V_{pmrs} e^{\Lambda_{pmrs}} \lambda_s^y \gamma_{ps} \gamma_{mr} \\ &\quad + 2V_{pmrs} e^{\Lambda_{pmrs}} \lambda_r^y \gamma_{mp} \gamma_{sr} - V_{pmrs} e^{\Lambda_{pmrs}} \lambda_r^y \gamma_{ps} \gamma_{mr} \\ &\quad - 4g_{pm}^y e^{\Lambda_{pm}} \lambda_r^y \lambda_m^y \gamma_{mp} \gamma_{rr} + 2g_{pm}^y e^{\Lambda_{pm}} \lambda_r^y \lambda_m^y \gamma_{pr} \gamma_{mr} \\ &\quad + 4g_{mq}^y e^{\Lambda_{mq}} \lambda_r^y \lambda_q^y \gamma_{qm} \gamma_{rr} - 2g_{mq}^y e^{\Lambda_{mq}} \lambda_r^y \lambda_q^y \gamma_{mr} \gamma_{qr} \\ &\quad - 2g_{pq}^y e^{\Lambda_{pq}} \gamma_{qp} \gamma_{mm} + g_{pq}^y e^{\Lambda_{pq}} \gamma_{pm} \gamma_{qm}. \end{aligned} \quad (\text{B4})$$

The gradient of orbital rotation κ_{ia} is the occupied-virtual block of the Fock matrix,

$$\frac{\partial E}{\partial \kappa_{ia}} = F_{ia}. \quad (\text{B5})$$

-
- [1] G. D. Mahan, *Many-particle physics*, 3rd ed. (Kluwer Academic, 2000).
- [2] C. Franchini, M. Reticioli, M. Setvin, and U. Diebold, Polarons in materials, *Nature Reviews Materials* **6**, 560 (2021).
- [3] D. N. Basov, A. Asenjo-Garcia, P. J. Schuck, X. Zhu, and A. Rubio, Polariton panorama, *Nanophotonics* **10**, 549 (2021).
- [4] A. S. Alexandrov and J. T. Devreese, *Advances in polaron physics*, Vol. 159 (Springer, 2010).
- [5] A. Mandal, M. A. Taylor, B. M. Weight, E. R. Koessler, X. Li, and P. Huo, Theoretical advances in polariton chemistry and molecular cavity quantum electrodynamics, *Chem. Rev.* **123**, 9786 (2023).
- [6] R. Bhuyan, J. Mony, O. Kotov, G. W. Castellanos, J. Gómez Rivas, T. O. Shegai, and K. Börjesson, The rise and current status of polaritonic photochemistry and photophysics, *Chem. Rev.* **123**, 10877 (2023).
- [7] B. S. Simpkins, A. D. Dunkelberger, and I. Vurgaftman, Control, modulation, and analytical descriptions of vibrational strong coupling, *Chem. Rev.* **123**, 5020 (2023).
- [8] K. Hirai, J. A. Hutchison, and H. Uji-i, Molecular chemistry in cavity strong coupling, *Chem. Rev.* **123**, 8099 (2023).
- [9] T. E. Li, B. Cui, J. E. Subotnik, and A. Nitzan, Molecular polaritons: Chemical dynamics under strong light-matter coupling, *Annu. Rev. Phys. Chem.* **73**, 43 (2022).
- [10] K. Nagarajan, A. Thomas, and T. W. Ebbesen, Chemistry under vibrational strong coupling, *J. Am. Chem. Soc.* **143**, 16877 (2021).
- [11] F. J. Garcia-Vidal, C. Ciuti, and T. W. Ebbesen, Manipulating matter by strong coupling to vacuum fields, *Science* **373**, eabd0336 (2021).
- [12] M. Ruggenthaler, D. Sidler, and A. Rubio, Understanding polaritonic chemistry from ab initio quantum electrodynamics, *Chem. Rev.* **0** (2023).
- [13] J. A. Hutchison, T. Schwartz, C. Genet, E. Devaux, and T. W. Ebbesen, Modifying chemical landscapes by coupling to vacuum fields, *Angew. Chem. Int. Ed.* **51**, 1592 (2012).
- [14] M. Hertzog, M. Wang, J. Mony, and K. Börjesson, Strong light-matter interactions: a new direction within chemistry, *Chem. Soc. Rev.* **48**, 937 (2019).
- [15] J. Bloch, A. Cavalleri, V. Galitski, M. Hafezi, and A. Rubio, Strongly correlated electron-photon systems, *Nature* **606**, 41 (2022).
- [16] W. Ahn, J. F. Triana, F. Recabal, F. Herrera, and B. S. Simpkins, Modification of ground-state chemical reactivity via light-matter coherence in infrared cavities, *Science* **380**, 1165 (2023).
- [17] J. J. Foley IV, J. F. McTague, and A. E. DePrince III, Ab initio methods for polariton chemistry, arXiv preprint arXiv:2307.04881 (2023).
- [18] B. M. Weight, X. Li, *et al.*, Theory and modeling of light-matter interactions in chemistry: current and future, arXiv preprint arXiv:2303.10111 (2023).
- [19] M. Ruggenthaler, J. Flick, C. Pellegrini, H. Appel, I. V. Tokatly, and A. Rubio, Quantum-electrodynamical density-functional theory: Bridging quantum optics and electronic-structure theory, *Phys. Rev. A* **90**, 012508 (2014).
- [20] C. Schäfer, F. Buchholz, M. Penz, M. Ruggenthaler, and A. Rubio, Making ab initio qed functional (s): Nonperturbative and photon-free effective frameworks for strong light-matter coupling, *Proc. Natl. Acad. Sci.* **118**, e2110464118 (2021).
- [21] I. V. Tokatly, Time-dependent density functional theory for many-electron systems interacting with cavity photons, *Phys.*

- Rev. Lett. **110**, 233001 (2013).
- [22] J. Flick and P. Narang, Ab initio polaritonic potential-energy surfaces for excited-state nanophotonics and polaritonic chemistry, *J. Chem. Phys.* **153** (2020).
- [23] J. Yang, Q. Ou, Z. Pei, H. Wang, B. Weng, Z. Shuai, K. Mullen, and Y. Shao, Quantum-electrodynamical time-dependent density functional theory within gaussian atomic basis, *J. Chem. Phys.* **155** (2021).
- [24] J. Yang, Z. Pei, E. C. Leon, C. Wickizer, B. Weng, Y. Mao, Q. Ou, and Y. Shao, Cavity quantum-electrodynamical time-dependent density functional theory within gaussian atomic basis. ii. analytic energy gradient, *J. Chem. Phys.* **156** (2022).
- [25] T. S. Haugland, E. Ronca, E. F. Kjørstad, A. Rubio, and H. Koch, Coupled cluster theory for molecular polaritons: Changing ground and excited states, *Phys. Rev. X* **10**, 041043 (2020).
- [26] A. F. White, Y. Gao, A. J. Minnich, and G. K. Chan, A coupled cluster framework for electrons and phonons, *J. Chem. Phys.* **153** (2020).
- [27] Y. Takada and A. Chatterjee, Possibility of a metallic phase in the charge-density-wave–spin-density-wave crossover region in the one-dimensional hubbard-holstein model at half filling, *Phys. Rev. B* **67**, 081102 (2003).
- [28] Y. Wang, I. Esterlis, T. Shi, J. I. Cirac, and E. Demler, Zero-temperature phases of the two-dimensional hubbard-holstein model: A non-gaussian exact diagonalization study, *Phys. Rev. Research* **2**, 043258 (2020).
- [29] J. Lee, S. Zhang, and D. R. Reichman, Constrained-path auxiliary-field quantum monte carlo for coupled electrons and phonons, *Phys. Rev. B* **103**, 115123 (2021).
- [30] B. M. Weight, S. Tretiak, and Y. Zhang, A diffusion quantum monte carlo approach to the polaritonic ground state, arXiv preprint arXiv:2309.02349 (2023).
- [31] E. Jeckelmann and S. R. White, Density-matrix renormalization-group study of the polaron problem in the holstein model, *Phys. Rev. B* **57**, 6376 (1998).
- [32] M. Tezuka, R. Arita, and H. Aoki, Density-matrix renormalization group study of pairing when electron-electron and electron-phonon interactions coexist: Effect of the electronic band structure, *Phys. Rev. Lett.* **95**, 226401 (2005).
- [33] B. Sandhoefer and G. K.-L. Chan, Density matrix embedding theory for interacting electron-phonon systems, *Phys. Rev. B* **94**, 085115 (2016).
- [34] T. E. Reinhard, U. Mordovina, C. Hubig, J. S. Kretzmer, U. Schollwöck, H. Appel, M. A. Sentef, and A. Rubio, Density-matrix embedding theory study of the one-dimensional Hubbard–Holstein model, *J. Chem. Theory Comput.* **15**, 2221 (2019).
- [35] F. Pavošević and A. Rubio, Wavefunction embedding for molecular polaritons, *J. Chem. Phys.* **157** (2022).
- [36] I. Lang and Y. A. Firsov, Kinetic theory of semiconductors with low mobility, *Sov. Phys. JETP* **16**, 1301 (1963).
- [37] R. Silbey and R. A. Harris, Variational calculation of the dynamics of a two level system interacting with a bath, *J. Chem. Phys.* **80**, 2615 (1984).
- [38] R. Silbey and R. A. Harris, Tunneling of molecules in low-temperature media: an elementary description, *J. Phys. Chem.* **93**, 7062 (1989).
- [39] R. Ramakumar and A. Das, Polaron cross-overs and d-wave superconductivity in hubbard-holstein model, *Eur. Phys. J. B* **41**, 197 (2004).
- [40] N. Rivera, J. Flick, and P. Narang, Variational theory of nonrelativistic quantum electrodynamics, *Phys. Rev. Lett.* **122**, 193603 (2019).
- [41] Y. Ashida, A. m. c. İmamoğlu, and E. Demler, Cavity quantum electrodynamics at arbitrary light-matter coupling strengths, *Phys. Rev. Lett.* **126**, 153603 (2021).
- [42] A. Mandal, S. Montillo Vega, and P. Huo, Polarized fock states and the dynamical casimir effect in molecular cavity quantum electrodynamics, *J. Phys. Chem. Lett* **11**, 9215 (2020).
- [43] R. R. Riso, T. S. Haugland, E. Ronca, and H. Koch, Molecular orbital theory in cavity qed environments, *Nat. Comm.* **13**, 1368 (2022).
- [44] M. Ruggenthaler, N. Tancogne-Dejean, J. Flick, H. Appel, and A. Rubio, From a quantum-electrodynamical light–matter description to novel spectroscopies, *Nat. Rev. Chem.* **2**, 1 (2018).
- [45] V. Rokaj, D. M. Welakuh, M. Ruggenthaler, and A. Rubio, Light–matter interaction in the long-wavelength limit: no ground-state without dipole self-energy, *J. Phys. B: At. Mol. Opt. Phys.* **51**, 034005 (2018).
- [46] A. Mandal, T. D. Krauss, and P. Huo, Polariton-mediated electron transfer via cavity quantum electrodynamics, *J. Phys. Chem. B* **124**, 6321 (2020).
- [47] C. Schäfer, M. Ruggenthaler, V. Rokaj, and A. Rubio, Relevance of the quadratic diamagnetic and self-polarization terms in cavity quantum electrodynamics, *ACS Photonics* **7**, 975 (2020).
- [48] M. A. D. Taylor, A. Mandal, and P. Huo, Resolving ambiguities of the mode truncation in cavity quantum electrodynamics, *Opt. Lett.* **47**, 1446 (2022).
- [49] A. Mandal, D. Xu, A. Mahajan, J. Lee, M. Delor, and D. R. Reichman, Microscopic theory of multimode polariton dispersion in multilayered materials, *Nano Lett.* **23**, 4082 (2023).
- [50] K. E. Cahill and R. J. Glauber, Ordered expansions in boson amplitude operators, *Phys. Rev.* **177**, 1857 (1969).
- [51] D. Cremer, Møller–Plesset perturbation theory: From small molecule methods to methods for thousands of atoms, *WIREs Comput. Mol. Sci.* **1**, 509 (2011).
- [52] Q. Sun, T. C. Berkelbach, N. S. Blunt, G. H. Booth, S. Guo, Z. Li, J. Liu, J. D. McClain, E. R. Sayfutyarova, S. Sharma, S. Wouters, and G. K.-L. Chan, PySCF: the Python-based simulations of chemistry framework, *WIREs Comput. Mol. Sci.* **8**, e1340 (2018).
- [53] Q. Sun, X. Zhang, S. Banerjee, P. Bao, M. Barbry, N. S. Blunt, N. A. Bogdanov, G. H. Booth, J. Chen, Z.-H. Cui, J. J. Eriksen, Y. Gao, S. Guo, J. Hermann, M. R. Hermes, K. Koh, P. Koval, S. Lehtola, Z. Li, J. Liu, N. Mardirossian, J. D. McClain, M. Motta, B. Mussard, H. Q. Pham, A. Pulkin, W. Purwanto, P. J. Robinson, E. Ronca, E. Sayfutyarova, M. Scheurer, H. F. Schurkus, J. E. T. Smith, C. Sun, S.-N. Sun, S. Upadhyay, L. K. Wagner, X. Wang, A. White, J. D. Whitfield, M. J. Williamson, S. Wouters, J. Yang, J. M. Yu, T. Zhu, T. C. Berkelbach, S. Sharma, A. Sokolov, and G. K.-L. Chan, Recent developments in the PySCF program package, *J. Chem. Phys.* **153**, 024109 (2020).
- [54] F. Pavošević, S. Hammes-Schiffer, A. Rubio, and J. Flick, Cavity-modulated proton transfer reactions, *J. Am. Chem. Soc.* **144**, 4995 (2022).
- [55] Q. Sun and G. K.-L. Chan, Exact and optimal quantum mechanics/molecular mechanics boundaries, *J. Chem. Theory Comput.* **10**, 3784 (2014).
- [56] H. Zhai and G. K.-L. Chan, Low communication high performance ab initio density matrix renormalization group algorithms, *J. Chem. Phys.* **154**, 224116 (2021).
- [57] H. Zhai, H. R. Larsson, S. Lee, Z.-H. Cui, T. Zhu, C. Sun, L. Peng, R. Peng, K. Liao, J. Tölle, *et al.*, Block2: a comprehensive open source framework to develop and apply state-of-the-art dmrg algorithms in electronic structure and beyond, arXiv preprint arXiv:2310.03920 (2023).
- [58] B. Gerlach and H. Löwen, Analytical properties of polaron sys-

- tems or: Do polaronic phase transitions exist or not?, *Rev. Mod. Phys.* **63**, 63 (1991).
- [59] K. Hannewald, V. Stojanović, J. Schellekens, P. Bobbert, G. Kresse, and J. Hafner, Theory of polaron bandwidth narrowing in organic molecular crystals, *Phys. Rev. B* **69**, 075211 (2004).
- [60] Y. Luo, B. K. Chang, and M. Bernardi, Comparison of the canonical transformation and energy functional formalisms for ab initio calculations of self-localized polarons, *Phys. Rev. B* **105**, 155132 (2022).
- [61] A. H. Al-Mohy and N. J. Higham, Computing the action of the matrix exponential, with an application to exponential integrators, *SIAM J. Sci. Comput.* **33**, 488 (2011).